The modal characteristics of high aspect ratio sailplane wings including the effects of bending and torsional rigidities

H Su[1,3] and J R Banerjee[2]

[1] Department of Engineering, University of Northampton, UK,
[2] Department of Mechanical Engineering & Aeronautics, School of Mathematics, Computer Science and Engineering, City, University of London, UK.
[3] Correspondence email address: huijuan.su@northampton.ac.uk

Abstract. The modal behaviour of two high aspect ratio sailplane wings with cantilever boundary conditions is investigated by applying the dynamic stiffness method and using the Wittrick-Williams algorithm as solution technique. The wing is idealised as an assembly of bending-torsional coupled beams for which the frequency dependent dynamic stiffness matrix is established. A Fortran computer program is developed to obtain the natural frequencies and mode shapes of the wings. The bending and torsional rigidities of each wing are varied and their subsequent effects on the natural frequencies and mode shapes are examined. A detailed parametric study with the variations of bending and torsional rigidities shows some interesting results which can be of practical help to the industry when designing such wings. The illustrative examples chosen for the baseline wings prior to changing their rigidities are representative of existing sailplanes. The results are presented and discussed and the paper concludes with some remarks.

1. Introduction

Sailplane wings are slender and flexible due to their high aspect ratios resulting from large spans and relatively short chords. As a consequence, they are easily prone to vibration problems. Modal analysis of sailplane wings is thus very important and plays an important role in their design. Analysis of this kind is an obligatory airworthiness requirement which is rigorously enforced by the civil aviation authorities. The purpose of this paper is to carry out such an analysis to predict the modal behaviour of sailplane wings by applying the dynamic stiffness method (DSM) and subsequently examining the effects of the wing rigidity properties on the modal characteristics. In order to provide the context of this research, interested readers may find references [1-6] useful as background studies.

One of the main motivations for modal analysis of aircraft wings originates from the fact that it is a fundamental prerequisite when carrying out the response analysis, particularly through the use of the normal mode method. It is well known that the finite element method (FEM) is generally used to solve such problems. Using the FEM, the stiffness and mass properties of all individual elements are assembled to form the overall stiffness and mass matrices of the structure. The typical eigenvalue problem is solved to provide the natural frequencies and the corresponding mode shapes of the structure upon imposing the boundary conditions. The FEM is numerically intensive and the degrees of freedom identified by the order of stiffness and mass matrices decide the number of eigenvalues, which are the natural frequencies. The higher order natural frequencies will be considerably less accurate. There is a powerful alternative to the FEM called the DSM for modal analysis of aircraft wings or other structures.

The DSM is based on an exact single dynamic stiffness element containing both the mass and stiffness properties of the element as the basic building block. The assembly procedure is the same as in the FEM, but a single dynamic stiffness element matrix is used for each structural component instead of separate mass and stiffness matrices to form the overall frequency-dependent dynamic stiffness matrix of the complete structure. The formulation in the DSM leads to a transcendental/nonlinear eigenvalue problem whereas a linear eigenvalue problem is generally encountered in the FEM. The best available solution technique to extract the eigenvalues in the DSM is to apply the Wittrick-Williams algorithm [7], which has received extensive coverage in the literature. The algorithm, which uses the Sturm sequence property of the dynamic stiffness matrix, is robust and ensures that no natural frequency of the structure is missed.

The paper focuses on the modal behaviour of two cantilever sailplane wings. The wings are idealised as an assembly of bending-torsional coupled beams [8-9]. The frequency dependent dynamic stiffness matrix of a bending-torsion coupled beam required for the analysis is outlined here. A computer program in Fortran is developed to obtain the natural frequencies and mode shapes of such wings using the Wittrick-Williams algorithm. The bending and torsional rigidities of each wing are then varied and their subsequent effects on the natural frequencies and mode shapes are investigated. A detailed parametric study with the variations of bending and torsional rigidities shows some interesting results which can be of practical help in the design of aircraft wings. The illustrative examples chosen for the baseline wings are representative of those of existing sailplane wings and the paper concludes with some remarks.

2. Theory

2.1. Formulation of dynamic stiffness matrix of a bending-torsional coupled beam

Figure 1 shows a bending-torsion coupled beam with length L, distance between the mass and elastic axes x_α, the bending and torsional rigidities EI and GJ respectively, the mass per unit length m, the polar mass moment of inertia per length about the Y-axis I_α. The bending displacement and torsional rotation are h and ψ. The coupled bending and torsional motions occur due to non-coincident mass and elastic axes which are respectively the loci of the centroid and shear centres of the beam cross-section. For an aircraft wing, it is not generally possible to realise a torsion-free bending displacement or a bending-free torsional rotation during its dynamic motion unless the load or the torque is applied through or about the shear centre. Given the perspective, a high aspect ratio non-uniform sailplane wing can be accordingly modelled as an assemblage of bending-torsion coupled beams. The representation in figure 1 is particularly relevant to analyse a high aspect ratio aircraft wing.

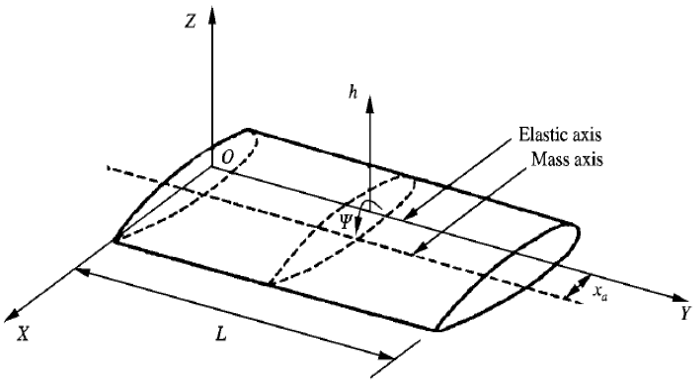

Figure 1. A wing idealised as a bending-torsion coupled beam.

The dynamic stiffness matrix of a uniform bending-torsion coupled beam has been established and extended to model a sailplane wing. The detailed procedure can be found in [8, 9]. The governing partial differential equations of motion for the beam with primes and over dots denoting partial differentiation with respect to position y and time t respectively are:

$$EIh'''' + m\ddot{h} - mx_\alpha\ddot{\psi} = 0 \quad (1)$$

$$GJ\psi'' + mx_\alpha\ddot{h} - I_\alpha\ddot{\psi} = 0 \quad (2)$$

For harmonic oscillation with circular frequency ω, the above differential equations can be solved using standard procedure [8, 9] to provide the solution for the amplitudes of both the bending displacement (H) and the torsional rotation (Ψ) in terms of six integration constants A_1 *to* A_6 as:

$$H(\xi) = A_1 cosh\alpha\xi + A_2 sinh\alpha\xi + A_3 cos\beta\xi + A_4 sin\beta\xi + A_5 cos\gamma\xi + A_6 sin\gamma\xi \quad (3)$$

$$\Psi(\xi) = A_1 k_\alpha cosh\alpha\xi + A_2 k_\alpha sinh\alpha\xi + A_3 k_\beta cos\beta\xi + A_4 k_\beta sin\beta\xi + A_5 k_\gamma cos\gamma\xi + A_6 k_\gamma sin\gamma\xi \quad (4)$$

where ξ is the non-dimensional length defined as $\xi = \frac{y}{L}$, and

$$\alpha = \left[2\left(\frac{q}{3}\right)^{\frac{1}{2}}\cos\left(\frac{\phi}{3}\right) - \frac{a}{3}\right]^{\frac{1}{2}},\ \beta = \left[2\left(\frac{q}{3}\right)^{\frac{1}{2}}\cos\left(\frac{(\pi-\phi)}{3}\right) + \frac{a}{3}\right]^{\frac{1}{2}},\ \gamma = \left[2\left(\frac{q}{3}\right)^{\frac{1}{2}}\cos\left(\frac{(\pi+\phi)}{3}\right) + \frac{a}{3}\right]^{\frac{1}{2}} \quad (5)$$

$$k_\alpha = \frac{b-\alpha^4}{bx_\alpha}, \quad k_\beta = \frac{b-\beta^4}{bx_\alpha}, \quad k_\gamma = \frac{b-\gamma^4}{bx_\alpha} \quad (6)$$

$$q = b + \frac{a^2}{3},\ \phi = cos^{-1}\left[\frac{27abc - 9ab - 2a^3}{\left\{2(a^2+3b)^{\frac{3}{2}}\right\}}\right],\ a = \left(\frac{I_\alpha\omega^2L^2}{GJ}\right),\ b = \left(\frac{m\omega^2L^4}{EI}\right),\ c = \left(\frac{I_\alpha - mx_\alpha^2}{I_\alpha}\right) \quad (7)$$

The expressions for bending rotation $\theta(\xi)$, bending moment $M(\xi)$, shear force $S(\xi)$ and torque $T(\xi)$ are given by [8, 9]

$$\theta(\xi) = \left(\frac{1}{L}\right)\{A_1\alpha sinh\alpha\xi + A_2\alpha cosh\alpha\xi - A_3\beta sin\beta\xi + A_4\beta cos\beta\xi - A_5\gamma sin\gamma\xi + A_6\gamma cos\gamma\xi\} \quad (8)$$

$$M(\xi) = -\left(\frac{EI}{L^2}\right)\{A_1\alpha^2 cosh\alpha\xi + A_2\alpha^2 sinh\alpha\xi - A_3\beta^2 cos\beta\xi - A_4\beta^2 sin\beta\xi - A_5\gamma^2 cos\gamma\xi - A_6\gamma^2 sin\gamma\xi\} \quad (9)$$

$$S(\xi) = \left(\frac{EI}{L^3}\right)\{A_1\alpha^3 sinh\alpha\xi + A_2\alpha^3 cosh\alpha\xi + A_3\beta^3 sin\beta\xi - A_4\beta^3 cos\beta\xi + A_5\gamma^3 sin\gamma\xi - A_6\gamma^3 cos\gamma\xi\} \quad (10)$$

$$T(\xi) = \left(\frac{GJ}{L}\right)\{A_1 k_\alpha\alpha sinh\alpha\xi + A_2 k_\alpha\alpha cosh\alpha\xi - A_3 k_\beta\beta sin\beta\xi + A_4 k_\beta\beta cos\beta\xi - A_5 k_\gamma\gamma sin\gamma\xi + A_6 k_\gamma\gamma cos\gamma\xi\} \quad (11)$$

Referring to figure 2, the boundary conditions for displacements are:

At $y = 0$ ($\xi = 0$): $H = H_1$, $\theta = \theta_1$, $\Psi = \Psi_1$ (12)

At $y = L$ ($\xi = 1$): $H = H_2$, $\theta = \theta_2$, $\Psi = \Psi_2$ (13)

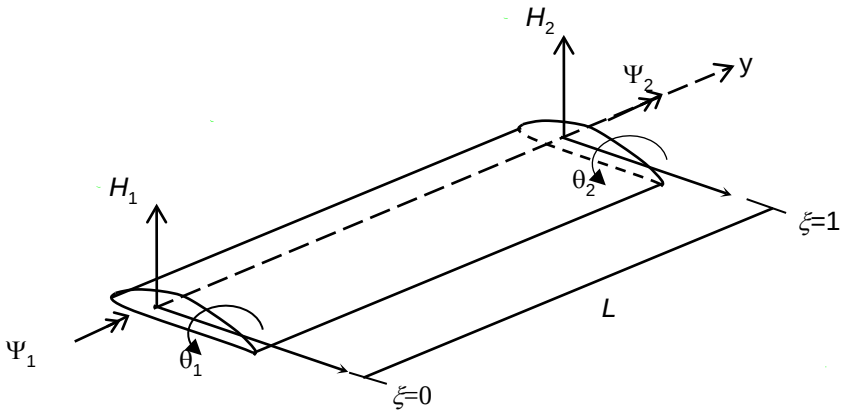

Figure 2. Boundary conditions for displacements of a sailplane wing element

Similarly referring to figure 3, the boundary conditions for the forces are:

At $y = 0$ ($\xi = 0$): $S = S_1$, $M = M_1$, $T = -T_1$ (14)

At $y = L$ ($\xi = 1$): $H = -S_2$, $M = -M_2$, $T = T_2$ (15)

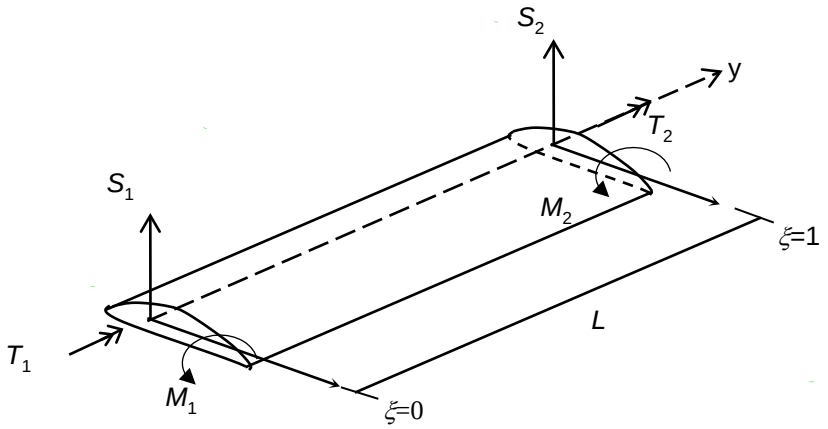

Figure 3. Boundary conditions for forces of a sailplane wing element

The expressions for displacements at the ends of the beam element can be obtained by applying the boundary conditions of equations (12) and (13) to equations (3), (4) and (8) to provide the following matrix relationship as:

$$\begin{bmatrix} H_1 \\ \theta_1 \\ \Psi_1 \\ H_2 \\ \theta_2 \\ \Psi_2 \end{bmatrix} = \begin{bmatrix} 1 & 0 & 1 & 0 & 1 & 0 \\ 0 & \alpha / L & 0 & \beta / L & 0 & \gamma / L \\ k_\alpha & 0 & k_\beta & 0 & k_\gamma & 0 \\ C_{h_\alpha} & S_{h_\alpha} & C_\beta & S_\beta & C_\gamma & S_\gamma \\ \alpha S_{h_\alpha} / L & \alpha C_{h_\alpha} / L & -\beta S_\beta / L & \beta C_\beta / L & -\gamma S_\gamma / L & \gamma C_\gamma / L \\ k_\alpha C_{h_\alpha} & k_\alpha S_{h_\alpha} & k_\beta C_\beta & k_\beta S_\beta & k_\gamma C_\gamma & k_\gamma S_\gamma \end{bmatrix} \begin{bmatrix} A_1 \\ A_2 \\ A_3 \\ A_4 \\ A_5 \\ A_6 \end{bmatrix} \quad (16)$$

or in matrix format as:

$$\boldsymbol{\Delta} = \mathbf{BA} \tag{17}$$

where **A** is the contact vector comprising the constants A_1 - A_6 and

$$C_{h\alpha} = \cosh\alpha;\ S_{h\alpha} = \sinh\alpha;\ C_\beta = \cos\beta;\ S_\beta = \sin\beta;\ C_\gamma = \cos\gamma;\ S_\gamma = \sin\gamma \tag{18}$$

The following matrix relationship can be obtained by substituting the boundary conditions of equations (14) and (15) for shear force, bending moment and torque into equations (9) - (11):

$$\begin{bmatrix} S_1 \\ M_1 \\ T_1 \\ S_2 \\ M_2 \\ T_2 \end{bmatrix} = \begin{bmatrix} 0 & W_3\alpha^3 & 0 & -W_3\beta^3 & 0 & -W_3\gamma^3 \\ -W_2\alpha^2 & 0 & W_2\beta^2 & 0 & W_2\gamma^2 & 0 \\ 0 & -W_1k_\alpha\alpha & 0 & -W_1k_\beta\beta & 0 & -W_1k_\gamma\gamma \\ -W_3\alpha^3S_{h_\alpha} & -W_3\alpha^3C_{h_\alpha} & -W_3\beta^3S_\beta & W_3\beta^3C_\beta & -W_3\gamma^3S_\gamma & W_3\gamma^3C_\gamma \\ W_2\alpha^2C_{h_\alpha} & W_2\alpha^2S_{h_\alpha} & -W_2\beta^2C_\beta & -W_2\beta^2S_\beta & -W_2\gamma^2C_\gamma & -W_2\gamma^2S_\gamma \\ W_1k_\alpha\alpha S_{h_\alpha} & W_1k_\alpha\alpha C_{h_\alpha} & -W_1k_\beta\beta S_\beta & W_1k_\beta\beta C_\beta & -W_1k_\gamma\gamma S_\gamma & W_1k_\gamma\gamma C_\gamma \end{bmatrix} \begin{bmatrix} A_1 \\ A_2 \\ A_3 \\ A_4 \\ A_5 \\ A_6 \end{bmatrix} \tag{19}$$

or in matrix format as:

$$\mathbf{F} = \mathbf{DA} \tag{20}$$

where

$$W_1 = \frac{GJ}{L},\ W_2 = \frac{EI}{L^2},\ W_3 = \frac{EI}{L^3} \tag{21}$$

The constant vector **A** can now be eliminated from equations (17) and (20) to give the following force-displacement relationship:

$$\mathbf{F} = \mathbf{K}\,\boldsymbol{\Delta} \tag{22}$$

where **K** is the 6×6 frequency dependent dynamic stiffness matrix given by

$$\mathbf{K} = \mathbf{D}\,\mathbf{B}^{-1} \tag{23}$$

The dynamic stiffness matrix in equation (23) representing a bending-torsion coupled beam such as an aircraft wing can now be used to model an aircraft wing.

2.2 Application of the Wittrick-Williams algorithm

The dynamic stiffness matrix in equation (23) can be used to compute the natural frequencies and mode shapes of a bending-torsion coupled beam. A non-uniform aircraft wing can be modelled as an assembly of many uniform bending-torsion coupled beams. For example, a non-uniform wing can be modelled as a stepped wing where it is split into a number of uniform elements. The dynamic stiffness matrices of all individual elements are assembled to form the overall dynamic stiffness matrix $\mathbf{K}_f$ of the complete wing. The natural frequency computation is accomplished by applying the Wittrick-Williams algorithm [7]. The algorithm monitors the Sturm sequence condition of $\mathbf{K}_f$ in such a way that there is no possibility of missing any natural frequency of the wing. The application procedure of the algorithm is briefly summarised here. Supposing that ω denotes the angular frequency of the vibrating wing, the number of natural frequencies passed (j) as ω is increased from zero to ω^* is given by

$$j = j_0 + \mathrm{s}\{\mathbf{K}_f\} \tag{24}$$

where $\mathbf{K}_f$, the overall dynamic stiffness matrix of the wing whose elements depend on ω is evaluated at $\omega = \omega^*$; s{$\mathbf{K}_f$} is the number of negative elements on the leading diagonal of $\mathbf{K}_f^\Delta$, $\mathbf{K}_f^\Delta$ is the upper triangular matrix obtained by applying the usual form of Gauss elimination to $\mathbf{K}_f$, and j_0 is the number of natural frequencies of the wing still lying between 0 and ω^* when the displacement components to which $\mathbf{K}_f$ corresponds are all zeros.(Note that the structure can still have natural frequencies when all its

nodes are clamped, because exact member equations allow each individual member to displace between nodes with an infinite number of degrees of freedom, and hence infinite number of natural frequencies between nodes. Thus

$$j_0 = \sum j_m \tag{25}$$

where j_m is the number of natural frequencies between 0 and ω^* for an individual component member with its ends fully clamped, while the summation extends over all members of the structure. Thus, with equations (24) and (25), it is possible to ascertain how many natural frequencies of the wing lie below an arbitrarily chosen trial frequency (ω^*). This feature of the algorithm can be used to converge upon any required natural frequency to any desired accuracy. As successive trial frequencies can be chosen, computer implementation of the algorithm is simple. For a detailed explanation and understanding of the Wittrick-Williams algorithm, readers are referred to the original work of Wittrick and Williams [7].

3. Results and discussion

Two sailplane wings with cantilever boundary conditions are analysed for their modal characteristics. The sailplanes are named as S_1 and S_2 to preserve commercial anonymity. The particulars for the two sailplanes are given in table 1. The unit for each parameter is provided in parentheses in the table.

Table 1. Particulars of the two sailplanes.

Parameters	Sailplane-S_1	Sailplane-S_2
Wing Span (m)	22	15
Wing Area (m^2)	15.44	10.05
Aspect Ratio	31.35	22.4
Wing Root Chord (m)	1.0	0.9
Wing Tip Chord (m)	0.4	0.4
Sweep angle (deg)	0	0
Fuselage Length (m)	7.6	6.72
Height Overall (m)	2.0	2.0
Weight Empty (kg)	390	234
Max Take-off weight (kg)	550	440
Max Wing Loading (kg/m^2)	37	36
Max Cruising Speed (knots)	135	105

A computer program in Fortran was developed to compute the natural frequencies and mode shapes of the wings using the dynamic stiffness method and the Wittrick-Williams algorithm. The first five natural frequencies and mode shapes of the two sailplanes are presented in table 2 and figure 4, respectively. In figure 4, the horizontal axis is the non-dimensional length (ξ) and the vertical axis is bending displacement (H) and/or the torsional rotation (Ψ). The letters B and T in table 2 indicate bending and torsion dominated modes, respectively whereas the letter C indicates a coupled mode which has substantial amount of both bending and torsional displacements.

Table 2. The natural frequencies of the two sailplane wings.

Category	Natural Frequencies (ω_i) (rad/s)				
	ω_1	ω_2	ω_3	ω_4	ω_5
Sailplane S1	10.64 (B)	42.62 (B)	109.6 (B)	111.5 (T)	201.4 (B)
Sailplane S2	13.38 (B)	42.09 (B)	93.35 (B)	164.2 (T)	167.4 (C)

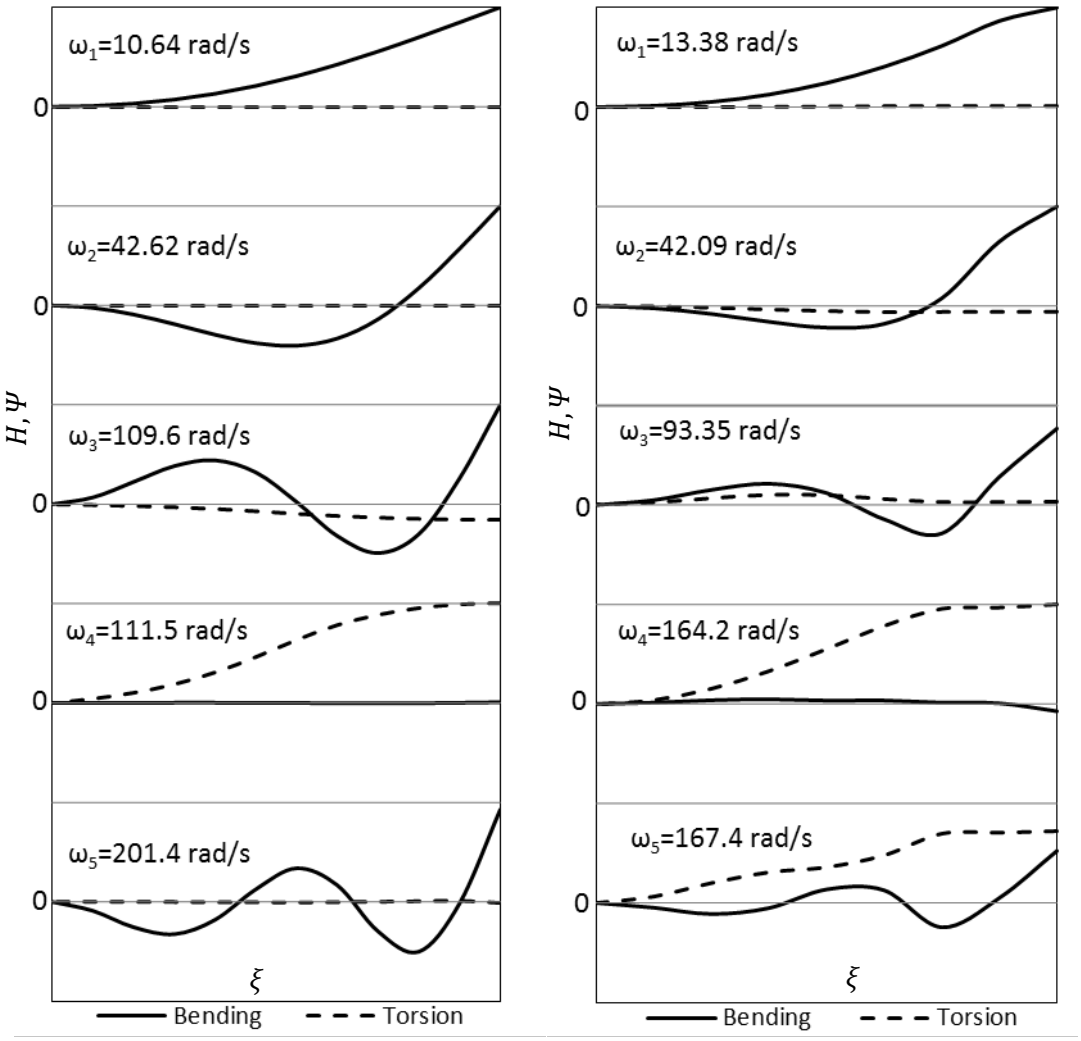

(a) Sailplane S1 (b) Sailplane S2

Figure 4. Natural frequencies and mode shapes of Sailplane wings S1 and S2.

A detailed parametric study with the variation of bending and torsional rigidities is then carried out. The bending (*EI*) and torsional (*GJ*) rigidities for each wing are varied between -25% to 25% with an increment of 5% in each step. Their subsequent effects on the natural frequencies and mode shapes are investigated. The first six natural frequencies with the variation of *EI* and *GJ* for S_1 are presented in tables 3 and 4 respectively. Clearly in table 3, all the natural frequencies corresponding to bending modes increase with the variation of the bending rigidity *EI* from -25% to +25% whereas the 6th one remains unchanged because it is a high frequency torsional mode which is not expected to change greatly as the torsional rigidity *GJ* is kept constant. Interesting results can be found in that there are modal interchanges (flip-over) for the variation of *EI* as the mode shapes changes from bending to torsional mode, see the 3rd natural frequency in table 3. Similar mode shape changes from torsional to bending mode can be found, for example in the 4th mode of table 3. With respect to the variation of *GJ* shown in table 4, the 1st, 2nd and 5th natural frequencies remain unchanged whereas the rest increase. Similar pattern can be observed that the 3rd and 4th modes are changed from torsional to bending mode and bending to torsion mode, respectively.

Table 3. The effects on the natural frequencies for S_1 with the variation of *EI*.

Variation in *EI* (%)	ω_i (rad/s)					
	ω_1 (B)	ω_2 (B)	ω_3	ω_4	ω_5 (B)	ω_6 (T)
-25	9.217	36.91	94.96 (B)	111.5 (T)	174.4	260.8
-20	9.519	38.12	98.07 (B)	111.5 (T)	180.1	260.8
-15	9.811	39.29	101.1 (B)	111.5 (T)	185.7	260.8
-10	10.10	40.43	104.0 (B)	111.5 (T)	191.1	260.8
-5	10.37	41.54	106.9 (B)	111.5 (T)	196.3	260.8
0	10.64	42.62	109.6 (B)	111.5 (T)	201.4	260.8
5	10.91	43.67	111.5 (T)	112.4 (B)	206.4	260.8
10	11.16	44.70	111.5 (T)	115.0 (B)	211.2	260.8
15	11.41	45.71	111.5 (T)	117.6 (B)	216.0	260.8
20	11.66	46.69	111.5 (T)	120.1 (B)	220.6	260.8
25	11.90	47.65	111.5 (T)	122.6 (B)	225.2	260.8

Table 4. The effects on the natural frequencies for S_1 with the variation of *GJ*.

Variation in *GJ* (%)	ω_i (rad/s)					
	ω_1 (B)	ω_2 (B)	ω_3	ω_4	ω_5 (B)	ω_6 (T)
-25	10.64	42.62	96.59 (T)	109.6 (B)	201.4	225.9
-20	10.64	42.62	99.76 (T)	109.6 (B)	201.4	233.3
-15	10.64	42.62	102.8 (T)	109.6 (B)	201.4	240.5
-10	10.64	42.62	105.8 (T)	109.6 (B)	201.4	247.4
-5	10.64	42.62	108.7 (T)	109.6 (B)	201.4	254.2
0	10.64	42.62	109.6 (B)	111.5 (T)	201.4	260.8
5	10.64	42.62	109.6 (B)	114.3 (T)	201.4	267.2
10	10.64	42.62	109.6 (B)	117.0 (T)	201.4	273.5
15	10.64	42.62	109.6 (B)	119.6 (T)	201.4	279.7
20	10.64	42.62	109.6 (B)	122.2 (T)	201.4	285.7
25	10.64	42.62	109.6 (B)	124.7 (T)	201.4	291.6

For the sailplane S_2, the first six natural frequencies with the variation of *EI* and *GJ* are presented in tables 5 and 6 respectively. Similar patterns, like the sailplane S_1, can be noted in respect of the modal interchanges (flip-overs), see the 4^{th} and 5^{th} modes.

It is well known that in flutter and response analysis of aeronautical and other structures, natural frequencies and mode shapes arising from the free vibration analysis play a very important role, particularly when the normal mode method is used. Essentially the mode shapes are appropriately scaled by the corresponding generalised coordinates when computing the flutter mode or the overall response of a structure such as an aircraft wing. The mode shapes provide essential information concerning the dynamic behaviour of a structural system and they are useful indicators of the properties of the system. It is also important to note that some of the modes can couple with each other which can give rise to instability, resulting in structural resonance causing eventual failure of the structure. In aeronautical applications, the presence of the aerodynamic forces alters the mode shapes significantly, triggering frequency coalescence phenomenon for which the classical bending-torsion flutter is a typical example. The importance of natural frequency and mode shape calculation cannot be overemphasised.

Table 5. The first six natural frequencies for S_2 with the variation of *EI* .

Variation in *EI* (%)	ω_i (rad/s)					
	ω_1 (B)	ω_2 (B)	ω_3 (B)	ω_4	ω_5	ω_6 (C)
-25	11.64	36.51	81.19	145.8 (B)	164.3 (T)	251.8
-20	11.97	37.69	83.66	149.9 (B)	164.3 (T)	259.3
-15	12.34	38.84	86.20	154.4 (B)	164.4 (T)	267.0
-10	12.69	39.96	88.65	158.7 (B)	164.5 (T)	274.5
-5	13.04	41.04	91.04	162.6 (B)	164.9 (T)	281.6
0	13.38	42.10	93.35	164.2 (T)	167.4 (C)	288.6
5	13.71	43.12	95.60	164.4 (T)	171.2 (C)	295.3
10	14.03	44.13	97.81	164.5 (T)	175.1 (C)	301.9
15	14.34	45.11	99.95	164.6 (T)	178.8 (C)	308.3
20	14.65	46.07	102.0	164.7 (T)	182.5 (C)	314.6
25	14.95	47.01	104.1	164.7 (T)	186.1 (C)	320.6

Table 6. The first six natural frequencies for S_2 with the variation of *GJ* .

Variation in *GJ* (%)	ω_i (rad/s)					
	ω_1 (B)	ω_2 (B)	ω_3 (B)	ω_4	ω_5	ω_6 (C)
-25	13.37	42.03	93.01	142.8 (T)	166.2 (C)	286.2
-20	13.38	42.04	93.10	147.3 (T)	166.5 (C)	286.8
-15	13.38	42.06	93.18	151.8 (T)	166.7 (C)	287.3
-10	13.38	42.07	93.24	156.1 (T)	166.9 (C)	287.8
-5	13.38	42.09	93.30	160.3 (T)	167.1 (C)	288.2
0	13.38	42.10	93.35	164.2 (T)	167.4 (C)	288.6
5	13.38	42.11	93.41	166.9 (C)	171.2 (T)	289.0
10	13.38	42.11	93.44	167.2 (C)	172.6 (T)	289.2
15	13.38	42.12	93.48	167.4 (C)	176.4 (T)	289.5
20	13.38	42.13	93.51	167.5 (C)	180.1 (T)	289.7
25	13.38	42.14	93.54	167.6 (C)	183.7 (T)	289.9

4. Conclusions

Using the dynamic stiffness method together with the Wittrick-Williams algorithm as the solution technique, the modal behaviour of two sailplane wings is investigated. Natural frequencies and mode shapes for these wings are presented and the results are examined and discussed. The bending and torsional rigidities of each wing are then varied and their subsequent effects on the natural frequencies and mode shapes are investigated. A detailed parametric study with the variations of bending and torsional rigidities provides some interesting results showing modal interchanges which can be of practical help in the design of such wings. The investigation paves the way for further research to establish trends for the modal behaviour of high aspect ratio sailplane wings.

References

[1] Banerjee JR 1984 *J. Aircraft* **21(9)** 733-5.
[2] Banerjee JR 1988 *J. Aircraft* **25(5)** 473-6.
[3] van Schoor M C and van Flotow AH 1990 *J. Aircraft* **27(10)** 901-8.
[4] Eslimy-Isfahany SHR, Banerjee JR and Sobey AJ 1996 *J. Sound and Vibration* **195(2)** 267-83.
[5] Tang D and Dowell EH 2001 AIAA **39(8)** 1430-41.
[6] Banerjee JR, Liu X and Kassem HI 2014 *J. Applied Nonlinear Dynamics*, **3(4)** 413-22.

[7] Wittrick WH and Williams FW 1971 Quarterly J. Mech;.and App. Mathematics **24(3)** 263-84.
[8] Banerjee JR 1989 Int. J. Numerical Methods in Engineering **28 (6)** 1283-98.
[9] Banerjee JR 1991 Adv. in Engineering Software, **13(1)** 17-24.